Direct evidence of ancient shock metamorphism at the site of the 1908 Tunguska event

Paola Vannucchi[1*], Jason P. Morgan[1], Damiano Della Lunga[1], Chris Andronicos[2], and W. J. Morgan[3]

[1]*Earth Sciences Department, Royal Holloway, University of London, UK.*

[2]*Earth, Atmospheric and Planetary Sciences Department, Purdue University, IN, USA.*

[3]*Department of Earth and Planetary Sciences, Harvard, Cambridge, MA, USA*

*Corresponding author

Abstract

Shock metamorphism is rarely found at the surface of the Earth. The most used structures to identify shock metamorphism are “true Planar Deformation Features” (PDFs) in quartz, now accepted as diagnostic indicators of a meteorite impact. Here we present several lines of evidence for shock metamorphism and PDFs developed in quartz occurring on samples centered on a circular geological structure on Mount Stojkovic (60º54’06"N; 101º55’40"E), which lies within southern surface exposures of the Siberian Traps. The shock event appears to have occurred during the eruption of the surface Siberian Traps basalts that cover this region. Curiously, Mount Stojkovic lies within ~3 km of the tree fall epicenter of the 1908 Tunguska event. Based on current estimates of the Phanerozoic impact distribution, there is at most a 1 in

~17,000 chance that the 1908 bolide would randomly fall on the site of a previous impact structure capable of creating shocked quartz. Just as improbable would be an airbust event, incapable of creating a small crater, that could have produced shock metamorphism. Our preferred least implausible hypothesis is that the shock-metamorphism here was associated with a terrestrial event, a hyperexplosive volcanic gas eruption called ‘Verneshot’.

1. Introduction

The 30 June 1908 Tunguska event flattened trees within a >2000 km^2 region (Vasilyev, 1998), and was associated with a seismic event (Ben-Menahem, 1975) and world-wide electromagnetic and atmospheric disturbances (Whipple, 1930). It is also linked to a unique period of ‘White Nights’ over Europe (Brauner, 1908), with the first white nights actually reported one day (Denning, 1908; Vasilyev, 1998) to one week (Vasilyev, 1998) before the 30 June event. Although it is generally accepted that the 1908 event was caused by a bolide explosion in the atmosphere 5-10 km above the Tunguska region, no unambiguous meteoritic material has ever been found near the epicenter of the treefall event, nor has a higher than Earth’s average amount of extraterrestrial dust (Vasilyev, 1998). It was not linked to a comet impact, as this should have led to at least a detectable regional ^{14}C spike (Liu et al., 2014), if not a larger global ^{14}C spike commensurate with the far-flung ‘White Nights’ dispersal of Tunguska material. The only proposed, and very controversial, crater is Lake Cheko (300 m diameter) which lies 8 km NNW of the epicenter (Gasperini et al., 2007; Collins et al., 2008; Gasperini et al., 2008).

In 1999, a Russian researcher presented an extended abstract indicating that she had found shocked quartz in samples collected on Mt. Stojkovic (Hryanina, 1999), close to the treefall epicenter (Fig. 1). This astounding claim was not accompanied by figures or other evidence to support her findings. We performed fieldwork in June 2008 and July 2009 in an attempt to replicate and better document her findings.

2. Geological background

The Mt. Stojkovic region was the focus of fieldwork in 2008 and 2009, because regional geologic maps indicate quartzose sandstone outcropping around the flanks of this hill. Mt. Stojkovic lies within a swampy ~10-km-wide depression known as the "Great Tunguska Depression" ringed by hills (Fig. 1A). Russian geologic maps interpret this depression as a volcanic center called Mt. Kulikovskii, which would be part of a bigger volcanic complex, Khushminskii, composed by several craters of Early Triassic age and associated with the Siberian Traps volcanism (Sapronov and Sobolenko, 1975; Sapronov, 1986). Mt. Stojkovic is interpreted as the remnant of one of the volcanic chimneys. Regional geologic maps show Mt. Stojkovic to be encircled by quartzose sandstone outcrops (Sapronov, 1986). Quartzose sandstone and conglomerate beds are pre-Siberian Trap continental deposits of Permian age (Sapronov and Sobolenko, 1975; Sapronov, 1986) that are interpreted to have been uplifted during the intrusion of the volcanic complex.

Almost the entire Great Tunguska Depression is covered either by taiga forest or by swamp. Outcrops are rare. Basaltic outcrops are present on Mt. Stojkovic, where there is also an outcrop of a poorly sorted deposit of sand and pebbles with blocks of up to ~m-size (Fig. 1B). We frequently used the common permafrost sampling technique of looking for rock fragments that are disinterred in the exposed roots of recent treefalls in the taiga forest. Trees root very poorly in the uppermost ~m of non-permafrost, thus treefalls containing rocks are fairly common. Although these rock fragments are not in place, they are: 1) a mixture of rounded and angular shaped fragments, 2) grouped in areas of homogeneous lithologies. These two characteristics give us confidence that rocks collected in treefalls have not experienced significant subaereal transport.

The new mapping confirms the existence of sandstone outcrops directly west of Mt. Stojkovic, where we found only dm-sized fragments of well-lithified quartzose sandstone to quartzite (Fig. 1B). On Mt. Stojkovic itself the sandstones are confined to a circular region near its summit (Fig. 1B). The high resolution mapping shows that the basaltic caprock in this region is essentially continuous except for a ~750 m diameter region near the summit of Mt. Stojkovic. In this region outcrops of basalt are completely absent. Instead, quartz-rich sand containing quartz pebbles and cobble sized fragments of quartzite are cropping out. Despite the variety in grain size, all the components of this deposit are well rounded. The deposit does not contain: 1) any basalt fragment or material of any size derived from weathering of basalt, 2) any bioclast. In this semi-circular region there is also the previously known "John's Rock" (Fig. 1B), a large boulder (~2 m * 2 m * 1.5 m) of quartzite with well-preserved sedimentary structures. The siliciclastic sediments are gray to pale pink in color and are characterized by laminations and graded bedding. Despite the limited size of the samples, some cm-scale thick and long cross sets are visible, as are parallel laminations. The composition and texture of this material is consistent with its source being the Permian deposits that underlie much of the Siberian Traps (Sapronov and Sobolenko, 1975; Sapronov, 1986). These siliciclastic strata have been described as being deposited in a continental environment in a variety of fluvial settings with predominant high-energy, braided systems.

The colloquial interpretation for John's Rock and the ~50 m diameter region surrounding it is that this is a recent glacial deposit. This is unlikely. Glaciologists, in fact, have shown that ice-sheets never covered this region; the southernmost extant of Central Siberian ice-sheets is believed to have been ~200 km to the north of Tunguska (Astakhov, 2004; Svendsen et al., 2004). In corroboration of this, there are no landforms typical of a formerly glaciated region in the vicinity of Mount Stojkovic. Furthermore, if it were glacial in origin, one would expect a moraine or drop deposit to contain abundant fragments of the Traps basalt that covers ~98% of the countryside between Tunguska and the icesheet's source region in the Putorana plateau (Astakhov, 2004; Svendsen et al., 2004) at the northern coast of Siberia. Such abundant mafic fragments are seen in the end-moraines that lie 200 km to the North of Tunguska (Astakhov, 2004), but are not found in the Mt. Stojkovic deposits.

The distribution of quartzite and basalt near the base of Mt. Stojkovic cannot exclude local downslope transport of quartzite from the John's Rock area. However on the western side of Mt. Stojkovic we only have found basalts (Fig. 1B). So there is no direct geologic evidence of downslope transport in this direction.

3. Analytical methods

We examined a total of 33 polished thin sections, 24 were quartzose sandstone/quartzite and 9 were basalt. We studied the samples under the optical (petrographic) microscope, a 4-axis universal stage, and a Scanning Electron Microscope (SEM) with Electron Back Scattered Diffraction (EBSD). SEM and EBSD analyses were made on carbon-coated thin sections and ultra-polished thin sections. SEM (instrument used at Modena and Reggio Emilia University: FEI Esem Quanta 200-FEI XL30 with a tungsten filament, micro analysis done with X-EDS Oxford INCA with a Si(Li) detector) was used to analyze the fabric of nanocrystalline samples and to make detailed compositional maps.

4. Deformation lamellae in quartz

The samples of lithic clasts and fragments collected at Mt. Stojkovic and to its west vary from quartzarenite (>90% quartz) to orthoquartzite (99%-100% quartz). At the mesoscopic scale, sedimentary structures are commonly preserved (Fig. 2A). At the microscopic scale, most of the quartz grains are single crystals. The quartzites are well cemented by secondary quartz overgrown on the individual grains. The overgrowths grew in optical continuity with the grains they nucleated from, but the original shape of the grain is revealed by thin impurity rims (Fig. 2B). Sand grains/quartz crystals are typically 1±0.5 mm. Static recrystallization is locally well developed as well as undulose extinction in the quartz crystals. Both mesoscopic and microscopic analysis– including thin section analysis with the R_f/Φ or the Fry methods (Ramsay and Huber, 1983) – on the shape and orientation of the individual grains does not indicate high bulk strain. Here the original shape and orientation of the grains forming the quartzite is not known, but a sedimentary fabric is present, and existed before deformation.

Individual quartz grains with usually one and more rarely two sets of deformation lamellae were identified as a feature in nearly all grains of 10 thin sections of quartzite (samples SQ(TU08/01), TU09/01, TU09/08, TU09/23, TU09/23bis, TU09/29a, TU09/30, TU09/30bis, TU09/31, TU09/31bis) (Fig. 2). The lamellae appear as sets of sharp parallel dark bands. Thickness and spacing of the individual bands are highly variable. Thickness ranges from 4-5 to 30 µm, and spacing from <10 µm to ~0.1 mm with an average of ~30µm. The shape is also variable from straight to curved. Many grains, though, have a highly heterogeneous distribution of bands, with areas characterized by high density lamellae. Examination by optical microscope shows that many of these bands contain fluid inclusions. Some bands only extend through portions of a grain of quartz, but often, the lamellae extend through the whole grain and into the quartz cement that surrounds the grains (Fig. 2A), indicating that the lamellae formed after the sandstone was cemented.

The crystallographic orientations of 100 lamellae sets in 100 grains were measured from sample SQ(TU08/01).

Figures 3A and 3B show the results of lamellae analysis. Plot A in Figure 3 shows that the distribution of quartz c-axes in these grains have a strong preferential orientation with angles between sets of 70°/110°. A plot of the great circle containing c and the pole to the lamellae (Fig. 3B) shows remarkable regularity with an evident tendency for the arrows to point toward a plane trending EW. Unfortunately the outcrop conditions did not allow the collection of oriented samples so that a full estimation of the stress field is not possible at this time.

The summary of PDF crystallographic orientations are reported in table 1, while the raw data are included in the supplementary material (Supplementary Material 1). To improve the reproducibility of the U-stage measurements we follow the recommendations by Ferrière et al. (2009). A histogram of angles between the c-axis and poles to the lamellae in quartz grains from sample SQ(TU08/01), in 5° bins, was built using the spreadsheet by Huber et al. (2011) and it is shown in Fig. 3C. Using a 5º error envelope on a Wulff net, 70% of measured lamellae correspond to specific crystallographic orientations: $\{10\bar{1}4\}$, $\omega\{10\bar{1}3\}$, and $\pi\{10\bar{1}2\}$. A significant number of data show polar angles lower than 17.62°. Indexing of crystallographic orientations has been performed here (Fig. 3C), but the reader should be aware that since the angles have been calculated based on only one set (the strongest visible set) of lamellae per quartz grain, indexing is not unequivocal as there is no unique azimuthal relationship within each grain.

The comparison of the histogram of Fig. 3C with histograms from the literature, for example French and Koeberl (2010), show a similar strong concentration of lamellae at specific planes with sharp peaks, a characteristic that has been recognized as a characteristic of “true” Planar Deformation Features – PDFs. In the case of the lamellae measured in sample SQ(TU08/01), though, the peak is centered at angles generally underrepresented in classical impact diagrams. For small angles, classic histograms populate the fields <6º and between 15º and 30º (French, 1998; French and Koeberl, 2010). Remarkably in sample SQ(TU08/01), lamellae parallel to the basal plane (0001), i.e. when the angle between the C-axis and lamellae pole is < 6º, are absent, while a relatively high proportion of lamellae poles lie between 8º and 15º from the C-axis.

The optical characteristics, the crystallographic orientations, and the shape of the frequency distribution of the lamellae in the Tunguska samples have many characteristics consistent with shock metamorphism. Ferrière et al. (2009) define that PFs (Planar Features that can be produced by tectonic deformation) are commonly oriented parallel to (0001) and {1011}, two planes that are not represented in our measurements. Furthermore the absence of PDFs parallel to the basal plane (0001) is commonly interpreted to indicate shock pressures higher than 10 GPa (Grieve et al., 1996). However the combination of angles shown in Figure 3C also suggests that the mechanism responsible for the Tunguska PDFs differs somewhat from that experienced in many other examples of ‘impact shock metamorphism’.

5. Other evidence for shock metamorphism

Optical microscope observations indicate that some of these quartz-rich samples also contain “toasted” quartz (French, 1998) (Sample TU09-31 in Figure 4A), silicic pseudotachylite veinlets (Sample TU09-29b in Figure 4B), spiky outgrowths of quartz and feldspar (mainly plagioclase) on clastic quartz and feldspar grains (Vernon, 2004) (Sample TU09-23 in Figure 4C), well-developed 'mosaic structures' (French, 1998) of individual grains, and siliceous spherulites. A back-scatter electron image of sample TU09-25 (Figure 4D) shows 'box-like' plagioclase (Osinski, 2003) which grew in the interstices between the spikes of the quartz and feldspars outgrowth. Figure 1B shows the distribution of these structures in samples collected in the mapped area.

We devoted particular attention to the spiky outgrowths. These structures are frequent in the Tunguska quartzites, and the samples show a variety of outgrowth intensities ranging from samples where the amount of outgrowths is minor, to samples where the sedimentary texture of the rock is completely overprinted by outgrowth textures. The spikes range from 50 µm to >1 mm in length and from 10 µm to 0.1 mm wide. A classic interpretation of the spiky outgrowths is that they are associated with rapid melting and quenching (Vernon, 2004). These characteristics are not compatible with the more slowly varying contact metamorphism that would be created by basalt emplacement.

Although not considered to be unique diagnostics for shock metamorphism (French and Koeberl, 2010), the presence of the features described above provides further evidence in support of the interpretation that shock metamorphism has affected the sedimentary rocks found at Mount Stojkovic.

None of the basalt samples that we examined show evidence of shock metamorphism, e.g. diaplectic basaltic glass, etc. The lack of shock metamorphism in the basalt implies that the shock event occurred before the final eruption stages of the local Siberian Traps.

6. What is the origin of shock metamorphism at Tunguska?

The shock metamorphism that we document here could not have been produced by any extraterrestrial-impact-linked hypothesis for the 1908 Tunguska event. There is no large crater. Furthermore, the fact that a few trees remained standing near the center of the region of knocked-down trees, and that these, and the knocked-down trees still had preserved bark is completely irreconcilable with the >10GPa shock metamorphism described above.

One hypothesis to explain this observation is that recent glacial processes transported the shocked rocks to this location. However, as discussed above, there is no evidence that glaciation ever extended into this region. Nor is there any local evidence of glaciation at Mt. Stojkovic.

Another hypothesis to explain this observation is that the 1908 airburst occurred over the site of a previous large impact that created the ~10 km Great Tunguska Depression (Hryanina, 1999), and that Mt. Stojkovic is the central uplift of this ancient impact event. However, the odds of this happening are extremely small. The odds are equal to the fraction of Earth's surface that has been hit by a previous ancient impact that made a crater large enough to be associated with shocked quartz. If we assume a minimum diameter for such craters that can produce shocked quartz of ~1 km, and the power-law size-frequency distribution of $N \propto D^{-1.8}$ (Grieve, 1984; Grieve and Pesonen, 1992), and a frequency D>20 km of 10^{-6}/250 Ma (Grieve, 1984), then we find that <0.006% of Earth's surface should be covered by post-Mesozoic impact features – in other words there is less than a 1 in 17,000 chance that a random bolide would have an airburst over the site of a previous large impact event that occurred within the past 250 Ma. Note that this estimate does not depend on how frequent airburst events are, as airburst events are much too small to create shock metamorphism by themselves. It only depends on the fractional area of Earth’s surface that has previously experienced a large enough impact to induce shock metamorphism. This is a conservative estimate because it assumes a higher impact frequency than most other studies have inferred. If a more conventional value for impact frequency is assumed (cf. discussion in Hughes, 1998) this would lead to an even smaller estimated probability of a modern airburst happening over a previous >1 km impact structure.

A third hypothesis is that the Great Tunguska Depression is indeed an ancient volcanic center associated with the Siberian Traps, but that this center was associated with a terrestrial shock-metamorphism event, a ‘Verneshot’ (Phipps Morgan et al., 2004). A Verneshot is a hypothesized kimberlite-pipe-like diatreme that forms during a hyperexplosive volcanic gas eruption. Mt. Stojkovic could therefore be the edifice created during this Verneshot event that happened during the rifting and flood basalt volcanism that was building the Siberian Traps. Although no kimberlites have been found in Tunguska, carbonatites have. The nearest known carbonatite (60°49’N, 101°53’E) (Pokrovskii et al., 2001) lies ~8 km south of the epicenter (Fig. 1A), and is thought to have formed at the time of the formation of the Siberian Traps (Pokrovskii et al., 2001). Relatively nearby, many other pipe-like structures (Svensen et al., 2009) and carbonatites (Pokrovskii et al., 2001) (Supplementary material 2) are also found, structures that we infer are also related to Siberian trap forming volcanism. In this scenario, the recent Tunguska event could then be a similar but much smaller terrestrial volcanic gas eruption linked to renewed plume activity and rifting in this region that is reusing the lithospheric pipe-of-weakness created during the Permian explosive event. This idea provides a potential explanation for why the 1908 Tunguska epicenter is essentially collocated with the center of the earlier megashock event.

Possible gas release structures were observed at the time of the 1908 Tunguska outburst. Local eyewitnesses reported that the event was associated with the appearance of dozens of new, ~50 m diameter, funnel-shaped ‘holes’ in the ground, as well as a larger (~1 km long) linear ‘tear in the ground’ (Kundt, 2001). These ‘holes’, now filled with water, are preferentially located in the lower, most swampy areas of the Great Tunguska Depression, and subsequent Russian geologists have referred to them as ‘volcanic craters’ (Sapronov and Sobolenko, 1975; Hryanina, 1999).

The idea that the continental lithosphere can have persistent zones of weakness predates Plate Tectonics. It also underlies the basic conception of the Wilson Cycle. Although the physical mechanisms remain very uncertain, it is also currently accepted that tectonic/volcanic episodes have often reoccurred at sites of rifting and volcanism. For example, this behavior is known to have happened along the Reelfoot Rift (Late Proterozoic) now co-located with the New-Madrid-Rough Creek-Mississippi Embayment (~90 Ma) rift/volcanic lineament (Ervin and McGinnis, 1975; Cox and Van Arsdale, 1997; McBride et al., 2003). Other examples include the Rio Grande Rift, the Oslo Graben, and the East African Rifts (Williams, 1982), the Benou Rift/Cameroon Line (Fitton, 1983), and the Baikal Rift system (Logatchev and Zorin, 1987). A possible explanation is that recurrent thermal anomalies are due to different plumes re-using the same drainage system at the base of the lithosphere, with plume material preferentially migrating along pathways where the lithosphere is already relatively thin.

A fourth possibility would be that the 1908 Tunguska event is terrestrial in origin, a volcanic gas eruption that reused the persistent lithospheric weakness created by a prior large bolide impact. This hypothesis seems more contrived to us, yet it also implies that a volcanic gas eruption was the source of the 1908 Tunguska event.

The findings above raise the possibility that the Tunguska region is the site of Earth's first reasonably well-documented hyperexplosive volcanic gas eruption. This explanation for the Tunguska events is consistent with several earlier suggestions that some sites with shocked quartz have a terrestrial origin (Bucher, 1963; McCall, 1964; Nicolaysen and Ferguson, 1990;

Luczaj, 1998) rather than being caused by an impact. It also shares elements of Kundt's (2001) proposal that the 1908 Tunguska event and other cryptoexplosions were caused by the ejection of high-pressure gases from below, and that they are related to the genesis of kimberlites. In summary, we think that Tunguska may hold an even bigger mystery than a recent bolide airburst – it may be the smoking gun that a Verneshot occurred here during the eruption of the Siberian Traps. In any case, we have confidently identified another major enigma associated with the site of the 1908 Tunguska event — namely what is the origin of the shock metamorphism found here?

Acknowledgements

This project has greatly benefitted from the help of many colleagues. Getting to this site would not have been possible without the logistical support from a 2008 Digital Ranch film project on the Tunguska event for the Discovery Channel, and a 2009 Veriscope Productions film project for the National Geographic Channel. We especially thank Susan Michaels (2008) and Dan Levitt and Rick Beyer (2009) for this critical support, with key field assistance from our Russian guides Andrei Chernikov and Andrei Y. In 2008, Pio Norelli of IGG-CNR Pisa interrupted his vacation to make the critical thin section that showed first evidence of shocked quartz PDFs, while Barbara Mader in Kiel University verified by electron microprobe that the rock was indeed 100% quartz. Rick Allmendinger at Cornell provided his U-stage microscope, shared his expertise in training Jason Phipps Morgan on the use of this instrument, and also made the measurements reported here on U-stage optical measurements of the PDFs. Andrey Brobov helped to access a key paper in the Russian literature. Lloyd White at Royal Holloway geolocated the map from Prokovskii et al. (2001) that is shown as Supplementary Figure 1. NSF provides partial support to operate the Bucknell EBSD facility (Chris Daniels), while Andronicos provided additional financial support for this analysis from Cornell University. We thank you all for your invaluable contributions to this effort.

All thin sections and samples are curated at the Earth Science Department of Royal Holloway, University of London

JPM and PV equally contributed to data acquisition, interpretation and writing of the paper. DdL and CA analysed the samples in thin section. JM contributed to the data interpretation.

References Cited

Astakhov, V., 2004, Middle Pleistocene glaciations of the Russian North: Quaternary Science Reviews, v. 23, p. 1285-1311.

Ben-Menahem, A., 1975, Source Parameters of the Siberian Explosion of June 30, 1908, from analysis and synthesis of seismic signals at four stations: Phys. Earth Planet. Int., v. 11, p. 1-35.

Brauner, B., 1908, The recent nocturnal glows: Nature, v. 78, p. 221.

Bucher, W. H., 1963, Are cryptovolcanic structures due to meteorite impact?: Nature, v. 197, p. 1241-1245.

Champagnon, B. et al., 1996, Raman study of quartz amorphization by shock pressure: Journal of Non-Crystalline Solids, v. 196, p. 221-226.

Collins, G. S. et al., 2008, Evidence that Lake Cheko is not an impact crater: Terra Nova, v. 20, no. 2, p. 165-168.

Cox, R. T., and Van Arsdale, R. B., 1997, Hotspot origin of the Mississippi embayment and its possible impact on contemporary seismicity: Engineering Geology, v. 46, p. 5-12.

Denning, W. F., 1908, The Sky Glows: Nature, v. 78, p. 247.

Ervin, C. P., and McGinnis, L. D., 1975, Reelfoot rift-reactivated precursor to the Mississippi Embayment: Geological Society of America Bulletin, v. 86, p. 1287-1295.

Ferrière, L. et al., 2009, Systematic study of universal-stage measurements of planar deformation features in shocked quartz: Implications for statistical significance and representation of results: Meteoritics & Planetary Science, v. 44, no. 6, p. 925-940.

Fitton, J. G., 1983, Active versus passive continental rifting: evidence from the West African rift system: Tectonophysics, v. 94, p. 473-481.

French, B. M., 1998, Traces of Catastrophe, Houston, Lunar Planetary Institute, 120 p.:

French, B. M., and Koeberl, C., 2010, The convincing identification of terrestrial meteorite impact structures: What works, what doesn't, and why: Earth-Science Reviews, v. 98, no. 1-2, p. 123-170.

Gasperini, L. et al., 2007, A possible impact crater for the 1908 Tunguska Event: Terra Nova, v. 19, p. 245-251.

Gasperini, L., Bonatti, E., and Longo, G., 2008, Lake Cheko and the Tunguska event: Impact or non-impact?: Terra Nova, v. 20, no. 2, p. 169-172.

Grieve, R. A. F., 1984, The impact cratering rate in recent time: J. Geophys. Res., v. 84, p. B403-B408.

Grieve, R. A. F., Langenhorst, F., and Stoffler, D., 1996, Shock metamorphism of quartz in nature and experiment .2. Significance in geoscience: Meteoritics & Planetary Science, v. 31, no. 1, p. 6-35.

Grieve, R. A. F., and Pesonen, L. J., 1992, The terrestrial impact cratering record: Tectonophysics, v. 216, p. 1-30.

Hryanina, L. P., 1999, The bouquet of the meteorite craters in the epicentre of Tunguska Impact 1908 year, Lunar and Planetary Science XXX: Houston, Lunar Planetary Institute.

Huber, M. S. et al., 2011, ANIE: A mathematical algorithm for automated indexing of planar deformation features in quartz grains: Meteoritics & Planetary Science v. 46, no. 9, p.

1418-1424.
Hughes, D. W., 1998, The mass distribution of crater-producing bodies, *in* Grady, M., Hutchison, R., McCall, G. J. H., and Rothery, D. A., eds., Meteorites: Flux with Time and Impact Effects, Volume 140: London, Geol. Soc. London, Special Publications, p. 31-42.
Kundt, W., 2001, The 1908 Tunguska catastrophe: An alternative explanation: Current Science, v. 81, p. 399-407.
Liu, Y. et al., 2014, Mysterious abrupt carbon-14 increase in coral contributed by a comet: Scientific Report, v. 4:3728.
Logatchev, N. A., and Zorin, Y. A., 1987, Evidence and causes of the two-stage development of the Baikal rift: Tectonophysics, v. 143, p. 225-234.
Luczaj, J., 1998, Argument supporting explosive igneous activity for the origin of "cryptoexplosion" structures in the midcontinent, United States: Geology, v. 26, p. 295-298.
McBride, J. H., Kolata, D. R., and Hildenbrand, T. G., 2003, Geophysical constraints on understanding the origin of the Illinois basin and its underlying crust: Tectonophysics, v. 363, p. 45-78.
McCall, G. J. H., 1964, Are cryptovolcanic structures due to meteoric impact: Nature, v. 201, p. 251-254.
Nicolaysen, L. O., and Ferguson, J., 1990, Cryptoexplosion structures, shock deformation and siderophile concentration related to explosive venting of fluids associated with alkaline ultranafic magmas: Tectonophys., v. 171, p. 303-305.
Osinski, G. R., 2003, Impact glasses in fallout suevites from the Ries impact structure, Germany: An analytical SEM study: Meteoritics and Planetary Science, v. 38, p. 1641-1667.
Ostroumov, M., Faulques, E., and Lounejeva, E., 2002, Raman spectroscopy of natural silica in Chicxulub impactite, Mexico: Comptes Rendus Geoscience, v. 334, no. 1, p. 21-26.
Phipps Morgan, J., Reston, T. J., and Ranero, C. R., 2004, Contemporaneous mass extinctions, continental flood basalts, and ‘impact signals’: Are mantle plume-induced ‘Verneshots’ the causal link?: Earth and Planetary Science Letters, v. 217, p. 263-284.
Pokrovskii, B. G. et al., 2001, Oxygen and carbon isotopic compositions of carbonatite-like rocks in the Tunguska syneclise: Petrology, v. 9, no. 4, p. 376-387.
Ramsay, J. G., and Huber, M. I., 1983, The techniques of modern structural Geology - Volume 1 : Strain Analysis., London, Academic Press, 307 p.:
Sapronov, N. L., 1986, Drevnye vulkanicheskie struktury na yuge tungusskoj sineklizy, Ancient volcanic structures on the south of the Tunguska synclinal (in Russian), Nauka, Novosibirsk.
Sapronov, N. L., and Sobolenko, V. M., 1975, Some features of geological structure of lower triassic Kulikovsky paleo-volcano, Problems of Meteoritics, , Nauka Publishers, Siberian Branch, p. 13-19.
Svendsen, J. I. et al., 2004, Late Quaternary ice sheet history of northern Eurasia: Quaternary Science Reviews, v. 23, p. 1229-1271.
Svensen, H. et al., 2009, Siberian gas venting and the end-Permian environmental crisis: Earth Planet. Sci. Lett., v. 277, p. 490-500.
Vasilyev, N. V., 1998, The tunguska meteorite problem today: Planet. Space Sci., v. 46, p. 129-150.
Vernon, R. H., 2004, A practical guide to rock microstructure, Cambridge, Cambridge University Press.

Whipple, F. J. W., 1930, The great Siberian meteor and the waves, seismic and aerial, which it produced: Q. J. Roy. Meteorol. Soc., v. 56, p. 287-304.
Williams, L. A. J., 1982, Physical aspects of magmatism in continental rifts, *in* Palmason, G., ed., Continental and oceanic rifts, Volume 8, AGU, p. 193-222.

Figure Captions

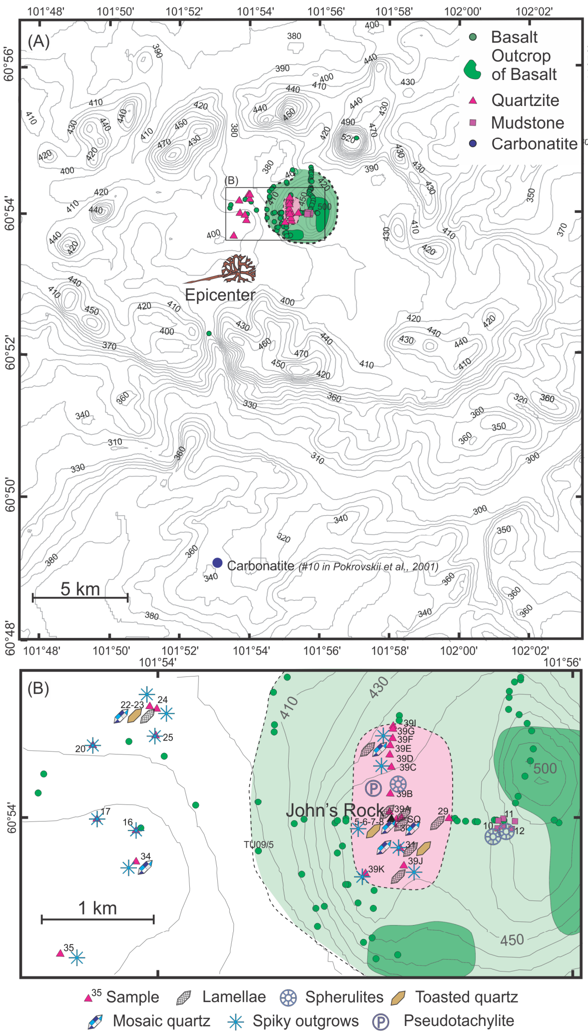

Fig 1.
Vannucchi et al.

Figure 1.

Maps of the "Great Tunguska Depression". (A) Topographic and geological map of the area around the tree-fall epicenter of the 1908 Tunguska event. Contour elevations in meters. Green circles represent samples of basalt, pink triangles represent quartzite and purple squares represent mudstone. The epicenter and the known carbonatite – blue circle (the reference number from Pokrovskii et al. 2001) - are also shown on the map region. (B) Zoom into the region around Mt. Stojkovic with newly collected quartzite (pink) and basalt (green) sample locations shown. Complete sample identification includes "TU09/", except for sample SQ, which is SQ(TU08/01).

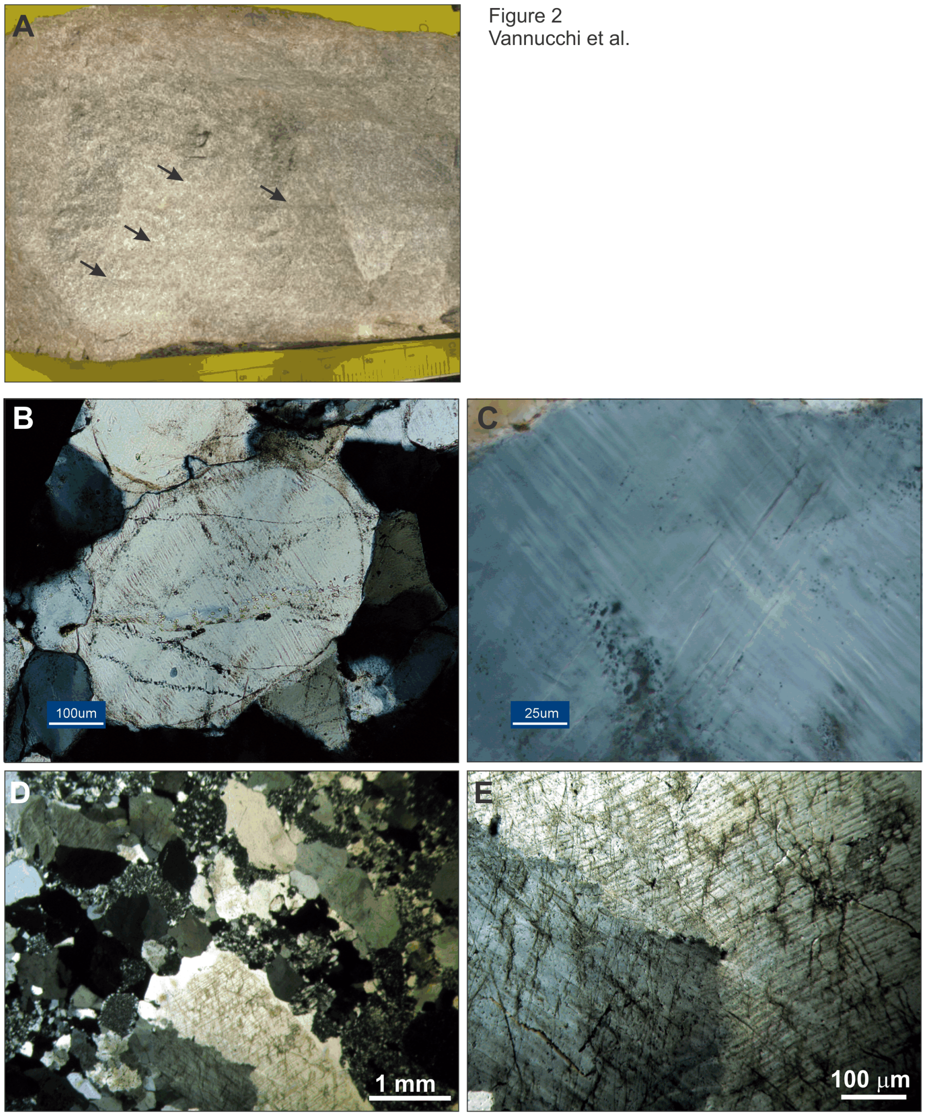

Figure 2.

Sample TU09/23, black arrows are showing parallel laminations in the quartzite. Microscopic features defining the shock metamorphic suite of the Tunguska quartzite samples. (A) Quartz grain in sample SQ(TU08/01) containing one set of deformation lamellae (crossed polarized light). The rim of the original clast and the cement overgrowth with deformation lamellae is visible. (B) two sets of deformation lamellae in a quartz grain from sample SQ(TU08/01). (C) Quartz grains in sample TU09/31 containing deformation lamellae (crossed polarized light). (D) Detail of deformation lamellae in sample TU09/31 (crossed polarized light).

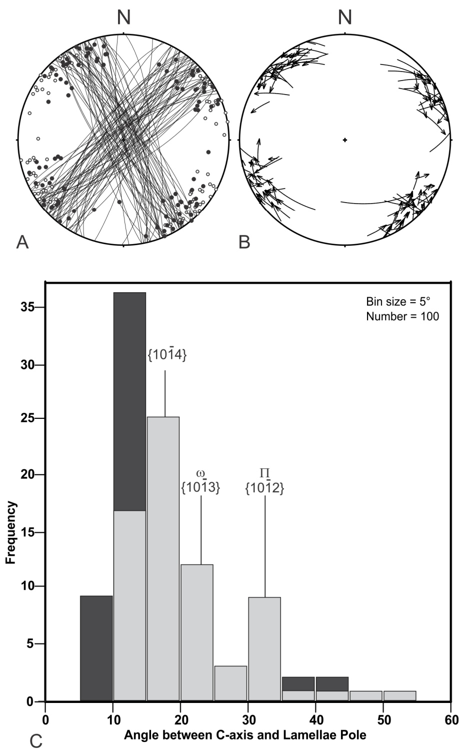

Figure 3. Vannucchi et al.

Figure 3.

Geometric characteristics of the planar deformation lamellae. (A) Lower hemisphere equal-area projection of quartz c-axes (solid circles) and deformation lamellae (PDFs) (open circles) for sample SQ. The great circles are the deformation lamellae themselves. (B) Lower hemisphere equal-area projection showing arcs of great circles connecting optic axes (tail) to pole to lamellae (head) for grains measured in sample SQ. (C) Histogram of orientation of deformation lamellae in sample SQ(TU08/01) showing the frequency distribution of the polar angle (angle between the C-axis of each quartz crystal and the lamellae pole). All measured PDF orientations are reported; “indexed” (gray) and “unindexed” (black) portions of the histogram bars are based on measurements using the Huber et al (2011) spreadsheet. Note that the unindexed PDF orientations are mainly concentrated with angles of 5–15° between the c-axis and poles to PDFs.

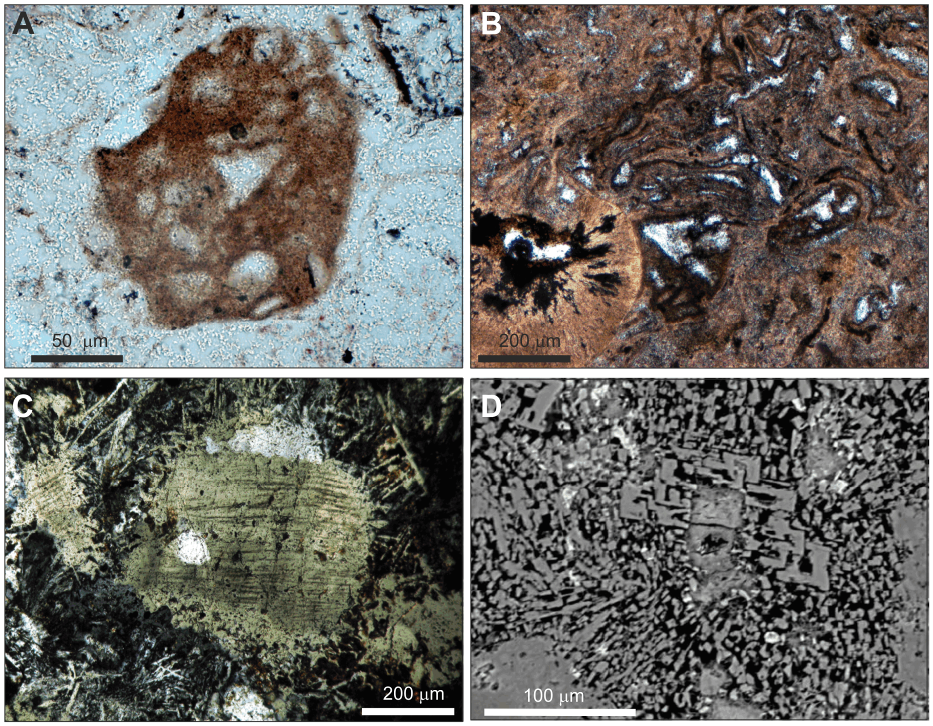

Figure 4
Vannucchi et al.

Figure 4.

(A) Grain of toasted quartz (plain polarized light) from sample TU09-31. (B) Pseudotachylite derived from quartzite, with a heterogeneous mixture of plastically deformed wallrock fragments (light-colored) mixed with discontinuous areas of lighter (silica rich) and darker (k-feldspar-rich), aphanitic material (Sample TU09-29b, plane polarized light). On the lower-left angle of the photograph is a spherulite consisting mainly of quartz with some alkali feldspar intergrowths. (C) Spiky outgrowths of quartz and feldspar (mainly plagioclase) on clastic quartz and feldspar grains (Sample TU09-23, crossed polarized light). At the center of the photograph is a shocked quartz clastic grain containing PDFs with extensive dendritic overgrowths of quartz and recrystallization of its boundaries. (D) Scanning electron back-scattered image of "box-like" plagioclase (Osinski, 2003) that has grown in interstices between the spikes (Sample TU09-25).

Table 1

Summary of PDF crystallographic orientations.

Table 1

No. of investigated grains	100
No. of measured sets	100
No. of PDF sets/grain	1

Miller-Bravais Indices *	**Absolute Frequency (%)**
c (0001)	0
e {1014}	37
ω {1013}	10
Π {1012}	13
r, z {1011}	1
m {1010}	0
ξ {1122}	2
s {1121}	0
ρ {2131}	0
x {5161}	0
a {1120}	0
{2241}	0
{3141}	0
t {4041}	0
k {5160}	0
Unindexed	30
Total	100

* The measured grains contain one PDF set, therefore indexing is not unique.

Supplementary material #1

Quartz deformation lamellae in sample SQ(TU08/01)

Def. Lamellae			C-axis		
obs T	obs P	Dir (N or S)	obs T	obs P	Dir (E or W)
11	14	s	108	17	w
148	10	n	51	4	w
119	9	n	21	12	e
150	6	n	42	5	e
147	15	s	48	8	e
132	9	s	29	4	e
138	14	s	40	0	e
29	2	n	129	3	w
141	20	s	356	41	e
34	2	n	147	10	e
153	4	n	51	33	w
128	12	n	26	4	w
140	14	s	40	21	e
158	15	s	61	25	e
20	7	s	112	25	e
33	13	s	129	28	w
137	8	s	40	30	e
142	20	s	37	13	e
124	7	n	22	7	w
125	8	s	27	10	e
33	3	n	133	11	e
140	6	s	45	24	w
20	10	s	106	38	w
20	6	s	119	13	w
116	11	s	13	7	e
38	6	n	155	22	e
28	7	s	118	24	w
15	0	n	113	3	e
43	10	s	145	10	w
23	6	n	104	36	w
22	2	s	127	6	w
127	1	n	24	14	w
31	2	s	133	7	w
125	11	n	18	20	w
149	3	n	46	12	w

133	15	s	29	18	e
137	2	s	37	11	w
359	20	s	104	16	w
25	14	n	125	18	e
164	8	n	63	21	w
147	2	s	45	5	w
34	9	n	133	4	e
32	5	s	138	26	e
131	10	s	35	5	e
152	1	s	49	9	e
11	1	s	111	5	e
136	6	n	35	7	w
10	0	n	111	12	e
13	15	s	82	20	e
139	15	n	44	30	e
135	13	s	33	32	e
118	8	s	12	10	w
126	17	s	23	1	e
153	5	s	60	14	e
27	10	s	115	24	e
40	10	s	142	2	w
128	2	n	24	6	e
135	5	s	45	31	w
126	6	s	12	18	w
21	10	n	121	2	e
3	5	n	113	27	e
12	10	s	116	8	w
138	7	n	35	11	w
135	1	s	43	21	e
119	9	s	197	6	e
199	14	s	125	7	e
35	3	s	134	11	e
22	0	n	121	12	e
40	6	n	148	24	e
27	18	s	157	29	w
35	17	n	135	8	e
35	16	n	131	27	e
124	13	n	15	27	w
33	20	s	134	13	w

142	5	s	38	7	w
32	9	s	133	8	w
148	17	n	39	10	w
193	7	n	109	23	w
120	20	n	11	18	w
22	11	s	120	20	w
147	12	s	46	18	w
134	8	n	19	22	w
15	21	n	117	21	e
133	22	s	212	11	w
202	6	s	134	30	e
32	11	s	134	15	w
153	9	s	47	15	e
144	4	n	51	13	e
125	4	e	22	12	n
41	16	s	145	19	w
142	0	n	45	3	w
14	26	s	105	33	w
127	7	s	27	1	w
157	25	s	54	21	e
127	16	n	200	9	e
32	12	s	133	16	w
140	8	n	31	18	w
143	21	s	43	14	e
190	12	s	109	6	w
24	12	n	123	10	e

Supplementary material #2

Location of carbonatite outcrops identified by Pokrovskii et al. (2001)

Sample	Latitude	Longitude
1	59.557653	100.042645
2	62.413006	101.535756
3a	63.150639	104.188855
3b	63.097101	104.361366
4	63.114947	100.810021
5	62.448698	101.714216
6	62.234547	105.455918
7	61.883576	104.617158
8	61.621835	103.683220
9	61.669425	101.000378
10	60.818767	101.886727
11	60.432105	101.886727
12	60.307183	101.975957
13	60.271491	99.1384490
14	60.402362	98.9064520
15	60.420208	99.0908600
16	60.087083	98.8886060
17	59.980007	98.5197900
18	60.319080	97.9249240
19	60.896100	96.7173480
Tunguska Shock Centre	60.901667	101.927778

Figure 1
Map view of location of carbonatite outcrops identified by Pokrovskii et al. (2001)

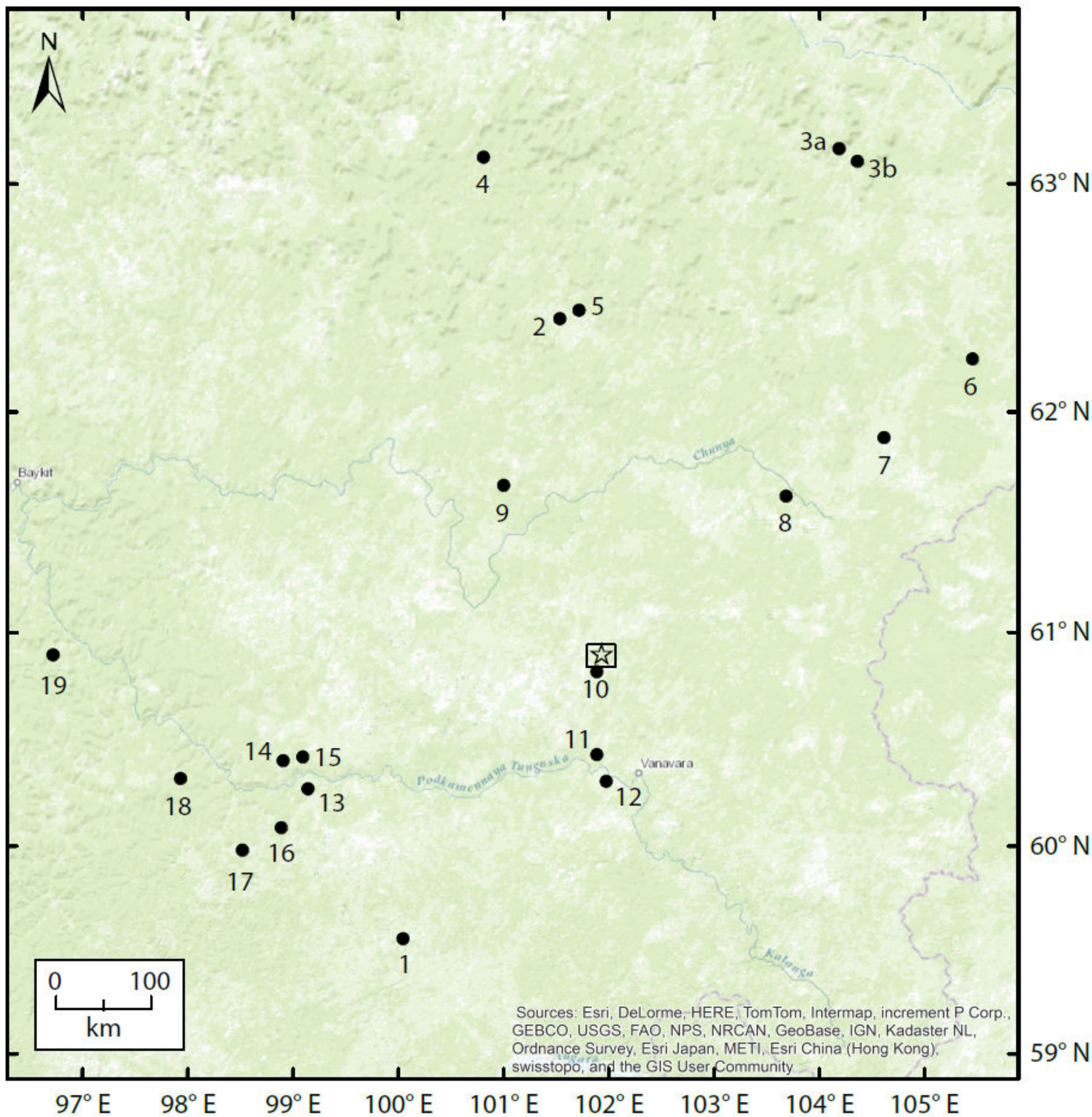

Pokrovskii, B. G., Vrublevskii, V. V., Sapronov, N. L., Parnachev, V. P., Moskalev, V. A., and Kudryavtsev, D. I., 2001, Oxygen and carbon isotopic compositions of carbonatite-like rocks in the Tunguska syneclise: Petrology, v. 9, no. 4, p. 376-387.